Acta Scientific Pharmaceutical Sciences

Volume 2 Issue 1 January 2018

Research Article

Molecular Spectroscopy Investigation on Pharmacodynamic Activity and Biological Property Analysis on Anti-Mycobacterial Drug; 4-Amino Salicylic Acid Using Computational Tools

R Aarthi[1], S Ramalingam[1]* and S Periandy[3]

[1]*Ph.D Scholar, Department of Physics, A.V.C. College, Mayiladuthurai, Tamilnadu, India*

[2]*Department of Physics, A.V.C. College, Mayiladuthurai, Tamilnadu, India*

[3]*Department of Physics, Kanchi Mamunivar Centre for PG studies, Puducherry, India*

***Corresponding Author:** S Ramalingam, Department of Physics, A.V.C. College, Mayiladuthurai, Tamilnadu, India.

Received: December 27, 2017; **Published:** January 11, 2018

Abstract

The Pharmacodynamic activity was keenly observed by recording FT-IR, FT-Raman, UV-Visible and NMR spectra of 4-Aminosalicylic acid. The observed absorption and scattering spectral sequence were analyzed to predict the role of compositional parts in the compound activity. The unknown physico-chemical properties were calculated and were correlated with the physical parameters. The drug activity of the compound was predicted by observing frontier molecular interaction profile. The electronic transitions among different energy levels of electronic structure were determined and hyperactive Polarizability causing the anti-micro bacterial activity was discussed. The exchange of chemical potential for creating drug potential by making transitions among non-bonding molecular orbitals has been examined. The QSAR properties were calculated and Lipinski's rules for drug likeness were reported and discussed to recognize the biological activity of the molecule. The VCD spectrum in different range of IR region for determining enantiomer ability was replicated at stable conformer and the hiding of toxicity was predicted.

Keywords: 4-Aminosalicylic Acid; Physico-Chemical; Hyperactive Polarizability; QSAR Properties; Lipinski's Rules; VCD Spectrum

Introduction

The salicylic acid is a derivative of carboxylic acid and it is widely used as an antimicrobial and antifungal agent in food industry [1,2]. In addition to that, the salicylic acid and its derivatives are acted as an intestinal antiseptic agent for the treatment of rheumatic fever [3]. In the past few decades, it is very important demanding for the pharmaceutical research community to fabricate new efficient antibacterial agents [4]. In order to resolve the serious task, the organic synthesize research is being carried out in the preparation of novel antibacterial agents against the challenge of the drug resistance. In this venture, it was found that, when the amino group is fused with aromatic ring structure in ortho, meta and para position, the spontaneous antibiotic character is induced.

Particularly, benzoic acid substituted with hydroxyl and amino groups in ortho and para locations is able to employ as an enriched anti-tuberculosis agent [5]. Thus, Amino salicylic acid is a biologically active compound and behaved as an anti-mycobacterial agent used with other anti-tuberculosis drugs (most often isoniazid) for the treatment of all forms of active tuberculosis due to susceptible strains of tubercle bacilli [6]. The two major considerations in the clinical pharmacology of amino salicylic acid are the prompt production of a toxic inactive metabolite under acid conditions and the short serum half-life of one hour for the free drug. Amino salicylic acid is bacteriostatic agent mycobacterium tuberculosis (prevent the multiplying of bacteria without destroying them). It also inhibits the onset of bacterial resistance to streptomycin and isoniazid [7,8]. It is also a safe and effective in the treatment of inflammatory bowel diseases.

In spite of its important anti-mycobacterial agent in anti-tuberculosis drug applications of 4-Amino salicylic acid, no work has been found to predicate the systematic investigation on the structure activity associated to its pharmaceutical potential. Therefore, the present investigation was made for the strong interpretation on the structure activity connected with the inducement of active drug property of the compound using spectroscopic data and computational results. In order to find the drug likeness of the present compound, the Lipinski's rules were verified. The QSAR properties were calculated and discussed to recognize the biological activity of the molecule.

Experimental Profile

Physical state

- As prepared compound is in solid phase which is found to be pure and spectroscopic grade.

Recording profile

- The FT-IR and FT-Raman spectra of the compound were recorded using a Bruker IFS 66V spectrometer and the instrument adopted with an FRA 106 Raman module equipped with aNd:YAG laser source operating at 1.064 µm line widths with 200 mW power [9].
- The high resolution ^{1}HNMR and ^{13}CNMR spectra were recorded using 300 MHz and 75 MHz FT-NMR spectrometer [10].
- The UV-Vis spectrum was recorded in the range of 200 nm to 800 nm, with the scanning interval of 0.2 nm, using the UV-1700 series instrument [11].

Computational profile

In order to design the structure precisely, calculate geometrical parameters, display the Mulliken charge levels, study the vibrational spectral properties, observe the molecular orbital interactions, examine the frontier molecular transitions on the electronic structure, the entire quantum chemical computations were performed using the Gaussian 09 D. 01.version software program in core i7 computer [12].

The computational calculations were performed over entire geometrical parameters, vibrational frequencies, simulation of molecular structure and spectra using B3LYP and B3PW91 methods adopted with 6-31++G(d,p) and 6-311++G(d,p) basis sets. The optimized molecular structure is presented in three different forms in the figure 1. The energy absorbance by the present compound related with electronic spectra, the NBO calculation are performed by using NBO 6.1 program and HOMO-LUMO depletion energies were calculated using time-dependent SCF method with best fit basis set. In the same way, the 1H and 13C NMR chemical shifts with respect to TMS were calculated by GIAO method using IEFPCM model in combination with B3LYP/6-311++G(2d,p). The Mullikan charge assignment on par with the compositional parts of molecule was calculated and was purposely used to elucidate for the determination of key factor for pharmaceutical activity of the compound. The dipole moment, linear polarizability and the first order hyper polarizability in multi coordinates of the compound were computed using B3LYP method with the 6-311++G(d,p) basis set. The thermodynamical functional values are calculated with the help of NIST program. The ECD and VCD spectra were simulated from available frequencies and the optical chirality was studied and the mechanism for masking the toxicity was interpreted.

Geometrical Parameters	Methods		
	HF	B3LYP	B3PW91
	6-311++G (d-p)	6-311++G (d-p)	6-311++G (d-p)
Bond length (Å)			
C1-C2	1.391	1.402	1.399
C1-C5	1.397	1.409	1.407
C1-C11	1.495	1.493	1.489
C2-C3	1.376	1.384	1.382
C2-H6	1.076	1.085	1.086
C3-H7	1.074	1.084	1.084
C3-C15	1.395	1.405	1.403
C4-C5	1.385	1.393	1.391
C4-H8	1.077	1.086	1.087
C4-C15	1.391	1.401	1.399
C5-O9	1.335	1.356	1.350
O9-H10	0.940	0.963	0.961
C11-O12	1.341	1.372	1.364
C11-O13	1.175	1.199	1.197
O12-H14	0.941	0.964	0.963
C15-N16	1.380	1.385	1.379
N16-H17	0.994	1.008	1.007
N16-H18	0.994	1.008	1.007
Bond angle (°)			
C2-C1-C11	117.59	117.464	117.50
C5-C1-C11	120.42	120.78	120.67
C1-C2-C3	121.87	121.64	121.72
C1-C2-H6	122.64	122.51	122.57
C3-C2-H6	119.04	119.00	118.96
C2-C3-7H	118.27	118.42	118.41
C2-C3-C15	120.40	120.28	120.29
H7-H3-C15	119.27	119.64	119.61
C5-C4-H8	120.31	120.05	120.09
C5-C4-C15	119.30	119.19	119.14
H8-C4-C15	121.00	121.21	121.30
C1-C5-C4	119.69	119.58	119.55
C1-C5-O9	120.43	120.45	120.35
C4-C5-O9	118.60	118.31	118.37
C5-O9-H10	120.93	121.19	121.23
C1-C11-O12	111.31	109.88	109.59
C1-C11-O13	114.92	114.93	114.73
O12-C11-O13	125.05	125.60	125.55
C11-O12-H14	119.98	119.43	119.68
C3-C15-C4	111.51	109.86	109.35
C3-C15-N16	119.03	118.68	118.64
C4-C15-N16	120.60	120.70	120.71
C15-N16-H17	120.32	120.56	120.59
C15-N16-H18	116.20	117.00	116.97
H17-N16-H18	116.58	117.48	117.47
Dihedral angles (°)			
C5-C1-C2-C3	0.3099	0.3269	0.287
C5-C1-C2-H6	178.3696	177.7485	177.622
C11-C1-C2-C3	-176.0374	-176.0688	-176.174
C11-C1-C2-H6	2.0223	1.3528	1.1601
C2-C1-C5-C4	0.5697	0.5872	0.6575
C2-C1-C5-O9	178.5877	178.5416	178.610
C11-C1-C5-C4	176.8605	176.9499	177.079
C11-C1-C5-O9	-5.1215	-5.0957	-4.9669
C2-C1-C11-O12	-42.7853	-40.3418	-40.6795
C2-C1-C11-O13	135.0503	137.6436	137.34
C5-C1-C11-O12	141.0269	143.4151	143.0101
C5-C1-C11-O13	-41.1375	-38.5995	-38.9704
C1-C2-C3-H7	178.3862	178.259	178.2206
C1-C2-C3-C15	-0.6757	-0.7336	-0.7541
H6-C2-C3-H7	0.3123	0.8232	0.8724
H6-C2-C3-C15	-178.7495	-178.1695	-178.1023
C2-C3-C15-C4	0.1593	0.2203	0.2683
C2-C3-C15-N16	178.0609	177.7999	177.8628
H7-C3-C15-C4	-178.9034	-178.7748	-178.7085
H7-C3-C15-N16	-1.0018	-1.1952	-1.114
H8-C4-C5-C1	179.393	179.1745	179.1518
H8-C4-C5-O9	1.4215	1.2798	1.258
C15-C4-C5-C1	-1.086	-1.1029	-1.1474
C15-C4-C5-O9	-179.0574	-178.9976	-179.0412
C5-C4-C15-C3	0.7094	0.6863	0.6707
C5-C4-C15-N16	-177.1984	-176.8968	-176.9269
H8-C4-C15-C3	-179.7714	-179.5922	-179.6298
H8-C4-C15-N16	2.3209	2.8247	2.7726
C1-C5-9O-H10	178.1019	179.9101	179.9585
C4-C5-O9-H10	-3.8903	-2.1514	-2.1072
C1-C11-O12-N14	-14.64	-12.275	-11.9412
O13-C11-O12-H14	167.4055	169.6057	169.9135
C3-C15-N16-H17	22.1929	20.667	20.6495
C3-C15-N16-H18	159.5085	161.4155	161.4659
C4-C15-N16-H17	-159.9326	-161.7989	-161.803
C4-C15-N16-H18	-22.617	-21.0503	-20.9866

Table 1: Optimized geometrical parameters for 4-Aminosalicylic acid computed at HF/DFT (B3LYP&B3PW91) with 6-311++G(d- p) basis sets.

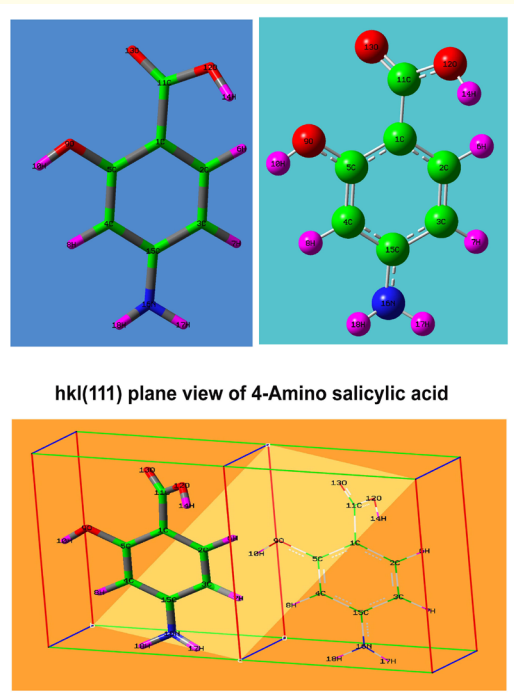

Results and Discussion

Molecular geometry deformation analysis

The molecular structure of the present molecule possesses bi-symmetry by which it belongs to C_{2V} point group symmetry. It was basically aromatic carboxylic acid derivatives and NH_2 present in ortho position, the OH was found to be substituted in meta position. Thus, the injected combinations formed 4-Amino salicylic acid and this molecule has low symmetry. Since the molecular structure is preserved by their hydrogen bonding around the ring, the ring property is conserved. But, here, the ring was substituted by OH, NH_2 and COOH groups on different positions. Accordingly, the hexagonal structure getting fractured intensively and its physical and chemical properties were to be altered and the modifications were pronounced by change of bond length and bond angles. In most of the cases, the substitution properties were dominated on the substituent and the entire base molecule properties are driven by ligand.

The acid group in the ring affected the C-C bond length was about 0.007Å whereas, the amino group was stressed the C-C bond length by 0.004Å. The hydroxyl group produced 0.009Å strain on CC of the ring. The bond length C1-C5 was identified to be stretched more than bond length C1-C2 since the existence of partial repulsive shearing forces. The outsized bond length of C1-C11 was observed as 1.493Å which was very large when compared with previous work [13]. From the evaluation of bond length system, it was observed that, the bond length profile of left moiety was more distorted than right moiety.

The highly stretched bond angle O12-C11-O13 was found as 125.60° in the acid group which was due to the bond length stretching for isolating the group to terminate the space charge induction. Such a type of rare induction among atoms was supported by the previous work on toluic acid [14]. The top moiety angle C2-C1-C5 was stretched more than bottom moiety C3-C15-C4 of the ring due to heavy substitutional injection. From the bond length and bond angle distortion reflected the impact of ligand over ring which showed the rate of involvement of ligand for the generation of drug property of product compound.

Mulliken charge distribution

The Mulliken charge distribution among the molecular orbital's usually used to describe the chemical equilibrium forces that polarized the electron clouds and their dynamic activity for generating the desired molecular chemical properties. The energy utilized by the molecular system is directly converted in the form chemical potential which established the assignment of nucleophilic and electrophilic profile over different components of the compound. Such a displayed wide range of charge spreading organized the active chemical potential mark on entire atoms of molecule which is the primary source that cause the desired drug property.

Here, the electrophilic and nucleophilic potential marks were found irrespective of base and ligand groups and showed in the figure 2. Here, the base was benzene and ligand groups were amine, acid and hydroxyl groups. The enriched electron clouds observed on N of amine group which was connected the C15, C3 and C2 of ring. Similarly, from O of hydroxyl group, the electron cloud actively moved to the C5 of ring. But, the electron cloud was found to be accumulated on COOH group itself. The displacement of electron clouds from amine, acid and hydroxyl groups were suddenly blocked by C1 of ring. Here, the C1 was a Y point junction of ring which making potential dipole and coupled the important functional group (COOH) with the ring. The zone around C1 is a charge depletion region due to which there were eight strong dipoles produced around the molecule. If the dipole production in the aromatic molecule is increased, the bio molecular property will be generated [15]. Here, the 80% of C-H as well as 20% of N-H dipole bonds generated consistent antibiotic property.

Thus, the chemical property of amine group was blended with the ring and the effect was extended over semicircle of ring and OH property was added with ring at the point of substitution. The property of COOH group was isolated from the ring which means that, the electron clouds pulled from the ring and thus the generated property due to the NH_2 and OH was controlled by the COOH group in the molecule. The ring core point C4 was almost neutralized, since the point at which the charges were pulled symmetrically by both groups. Such a push and pull of molecular charges from ligand to ring and from ring to ligand produced potential drug quality in the molecule.

Molecular property analysis

The results obtained from predicted Lipinski's parameters and other drug-likeness molecular properties of title compound using HyperChem 8.0.6 software were presented in table 2. The results of bio activity parameters were calculated using Molinspiration online database. The topographical polar surface area and lipophilicity diagrams of present compound were exhibited in figure 3. The calculated results exposed that, the present compound obsessed drug-like properties based on Lipinski's rule of five. In addition to that, the supporting parameters were predicted the drug quality. The Lipinski rule of five is generally used to evaluate drug likeness and also used to determine whether the chemical compound has a definite pharmacological or biological activity to fabricate an oral active drug [16,17].

Lipinski's parameters	Values
Hydrogen bond donor count	3
Hydrogen bond acceptor count	4
Rotatable bond count	1
Topological Polar Surface Area	83.55 A^2
Molecular mass and MW	153.14 g/mol
Exact Mass	153.135 g/mol
Heavy Atom Count	4
Covalently-Bonded Unit Count	4
Log p	0.92
N atoms	83.55
n ON	4
n OHNH	4
n violations	0
nrotb	1
Molecular Volume	130.35
GPCR ligand	-0.79
Ion channel modulator	-0.23
Kinase inhibitor	-0.79
Nuclear receptor ligand	-0.87
Protease inhibitor	-0.86
Enzyme inhibitor	-0.16
Drug-likeness score	0.16- -0.87

Table 2: Physical parameters of 4-Aminosalicylic acid.

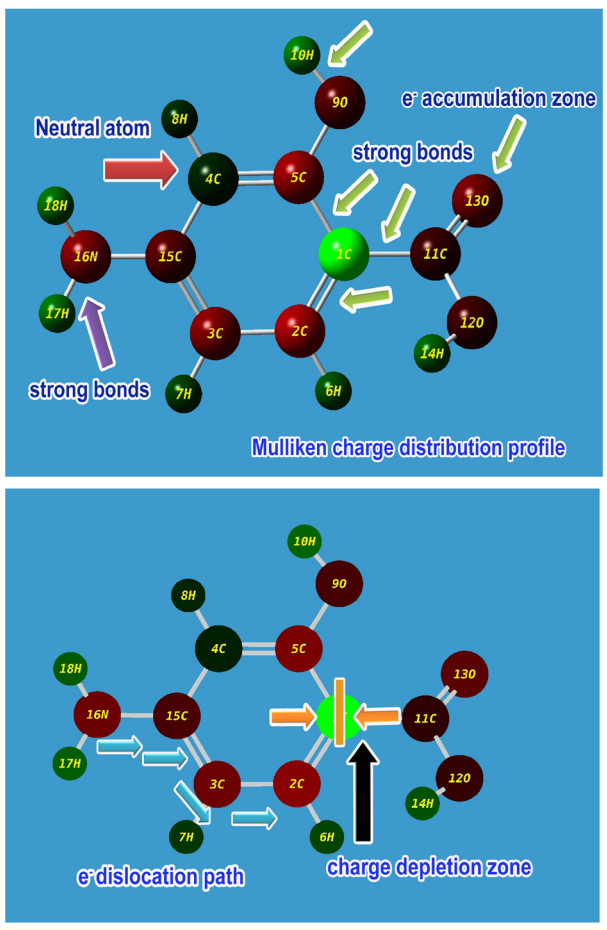

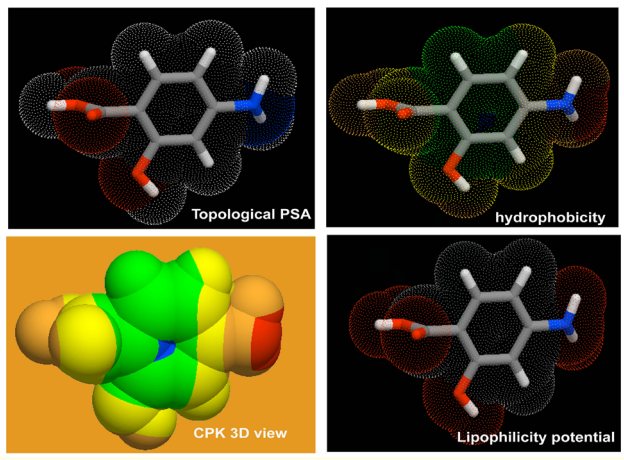

If the aromatic compound is to be drug like and orally bio available, its molecular weight should be ≤ 500, the Log P ≤ 5, Hydrogen bond acceptor ≤ 10 and Hydrogen bond Donor ≤ 5 [18]. In this case, the MW- 153.14, Log p- 0.92, HBA-4 and HBD-3 which showed that, the present molecule possessed physico chemically significant descriptors and pharmacokinetically related properties. Generally, if the molecule having the rotatable bonds ≤ 10 and total polar surface area ≤ 140 A2, the compound has membrane permeability and oral bio availability [19]. In the case of 4-Aminosalicylic acid, the RB and TPSA were observed to be 1 and 83.55 A^2 respectively. Thus, the present chemical compound could have good aqueous-solubility and efficient to penetrate the membranes of kidney.

The Lipinski rule of five is significant and is considered prognostic for enriched bioavailability; normally, of the 100%, the 20% of oral drugs disobey at least one of the criterion and 10% not succeed in two or three [20]. In this case, all the five rules have been satisfied through which the present compound having improved membrane permeability and fine intestinal availability. The heavy atom count and Covalently-Bonded Unit Count of the title compound was determined to be 4 and 4 respectively. Such the values ensure the covalent character of the compound and the presence of heavy atom was N and O which emphasized the antibiotic activity of the compound. The drug likeness score was determined as -0.16 – -0.87 for the present case. Though the parameter range was observed to be negative, it was located in acceptable region. This view of molecule designated the compound as a new drug candidate with high transport quality.

The G protein–coupled receptors (GPCRs) also called as seven-transmembrane domain receptors and it has been calculated to be 0.79 for the present molecule. From this observed value, it was clear that; good signal transduction can be taking place without annihilation. The Ion channel modulator value was found to be 0.23 and this value of present case is good for the modulation by which the Ion channels were pore-forming membrane proteins, permits ions to flow through the channel pore. The kinase inhibitor of present case was 0.79 which was adequate to make the penetration power and modulate its function of protein kinases in good condition. The nuclear receptors are multifunctional protein which plays key roles in both embryonic development and adult homeostasis which was found to be 0.87 and it was available with plenty of ligand concentration to trans-conductance the electrical signals of their equivalent ligands. The Protease inhibitor is an antiviral intensification of the prepared molecule and was found to be 0.86 for the title molecule. Though the observed value was rather low, the present compound will be acting as antibiotic drug.

Vibrational profile

The IR and Raman spectral pattern is not only used for the structure elucidation analysis, it also used for the knowing the dynamical parts of the aromatic molecule. Usually, the aromatic complex was fabricated by the combinations of base and ligand groups and it is tailored for getting desired chemical properties. In this scheme, the rate of operating mechanism constructed in the molecule is very significant to determine of role of entities causing directly to generate the particular drug property. With the intention of describing the drug mechanism, it is necessary to identify the dynamic component of the molecule. This branch can be studied by the help of observation of fundamental frequency pattern which to be satisfied the characteristic region of the each and individual bonds of molecule.

Accordingly, fundamental and group frequencies of present aromatic complex of 4-Aminosalicylic acid have been assigned with respect to the expected region with accurate wavenumber. Since the molecule belongs to C_s point group of symmetry, the fundamental vibrations have been divided as 48 vibrations. Out of that fundamental vibrations of the present molecule are distributed as 33 in plane vibrations denoted by A' species and 15 out of plane vibrations denoted by A" species, i.e., $_{vib}$ = 33A'+ 15A"

For studying the dynamic activity of the bonds and bond angles, the FT-IR and FT-Raman frequencies were calculated at HF and hybrid theories; B3LYP and B3PW91 with appropriate basis sets; 6-31++G(d,p) and 6-311++G(d,p) were presented in table 3. The vibrational pattern scanned and simulated FT-IR and FT-Raman spectra were depicted in the figure 4 and 5 respectively

S. No	Symmetry Species C_s	Observed frequency (cm^{-1})		Methods			Vibrational Assignments
				HF	B3LYP	B3PW91	
		FT-IR	FT-Raman	6-311++G (d,p)	6-311++G (d,p)	6-311++G (d,p)	
1	A′	3450m	-	3632	3616	3356	(O-H)υ
2	A′	3445m	-	3630	3594	3395	(O-H)υ
3	A′	3300m	-	3393	3383	3300	(N-H) υ
4	A′	3290m	-	3302	3164	3229	(N-H) υ
5	A′	3000s	-	3000	3001	3002	(C-H) υ
6	A′	2990s	-	3164	2984	2984	(C-H) υ
7	A′	2985s	-	3149	2966	2967	(C-H) υ
8	A′	1610s	-	1575	1610	1606	(C=O)υ
9	A′	1600s	1600s	1572	1600	1576	(C=C) υ
10	A′	1570s	-	1555	1570	1557	(C=C) υ
11	A′	-	1550m	1526	1550	1535	(C=C) υ
12	A′	1530m	-	1599	1530	1530	(C-C) υ
13	A′	1510w	-	1520	1510	1520	(C-C) υ
14	A′	1470s	-	1475	1470	1475	(C-C) υ
15	A′	1450s	1450vs	1465	1450	1460	(O-H) δ
16	A′	-	1395vs	1450	1400	1508	(O-H) δ
17	A′	1390vs	-	1390	1390	1382	(N-H) δ
18	A′	1385s	-	1385	1385	1316	(N-H) δ
19	A′	1315s	1315m	1315	1315	1305	(C-N) υ
20	A′	1290m		1290	1290	1295	(C-C) υ
21	A′	1250s	1250s	1255	1250	1260	(C-O) υ
22	A′	1170m	1170w	1122	1170	1151	(C-O) υ
23	A′	1150vw	1150w	1098	1150	1140	(C-H) δ
24	A′	-	1060s	1032	1065	1090	(C-H) δ
25	A′	-	950vw	917	950	1081	(C-H) δ
26	A′	-	915m	915	939	929	(C-H) δ
27	A′	880w	-	861	932	924	(O-H) γ
28	A″	-	875m	875	885	883	(O-H) γ
29	A″	-	855s	851	873	869	(N-H) γ
30	A″	850m	850s	893	861	859	(N-H) γ
31	A″	840m	-	852	800	795	(C=O) δ
32	A″	790m	-	789	739	735	(C-H) γ
33	A″	-	780s	712	688	682	(C-H) γ
34	A″	-	750s	684	660	655	(C-H) γ
35	A′	685m	-	630	608	603	(C-O) δ
36	A′	-	615vw	604	577	584	(C-O) δ
37	A′	-	500w	488	534	527	(C-N) δ
38	A′	-	490m	481	525	518	(CCC) δ
39	A′	-	410m	403	406	404	(CCC) δ
40	A′	360m	-	360	407	405	(CCC) δ
41	A′	310w	310w	318	319	322	(C-COOH) δ
42	A″	300w	-	313	298	303	(CCC)γ
43	A″	280w	-	296	289	287	(CCC)γ
44	A″	210w	210w	208	213	214	(CCC)γ
45	A″	180w		185	184	187	(C-O) γ
46	A″	-	150w	151	155	155	(C-O) γ
47	A″	110w	-	109	76	101	(C-N) γ
48	A″	90w	-	69	51	67	(C-COOH) γ

Table 3: Observed and HF and DFT (B3LYP & B3PW91) with 6-311++G (d,p) level. Calculated vibrational frequencies of 4-Aminosalicylic acid.

VS: Very strong; S: Strong; m- Medium; w: Weak; as: Asymmetric; s: Symmetric; υ: Stretching; α: Deformation; δ: In plane bending; γ: Out plane bending; τ: Twisting

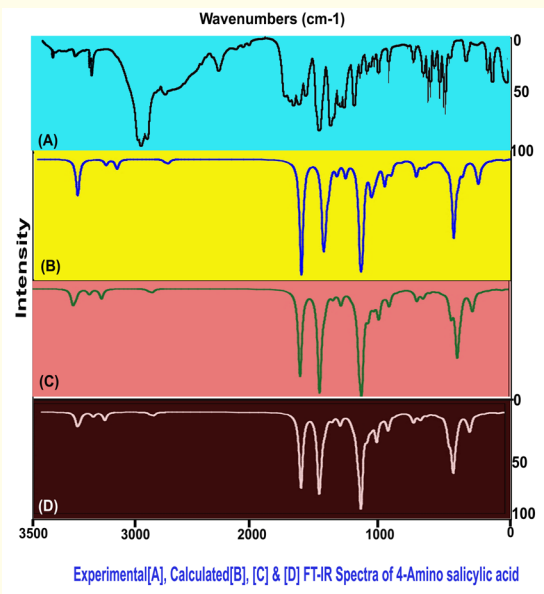

Experimental[A], Calculated[B], [C] & [D] FT-IR Spectra of 4-Amino salicylic acid

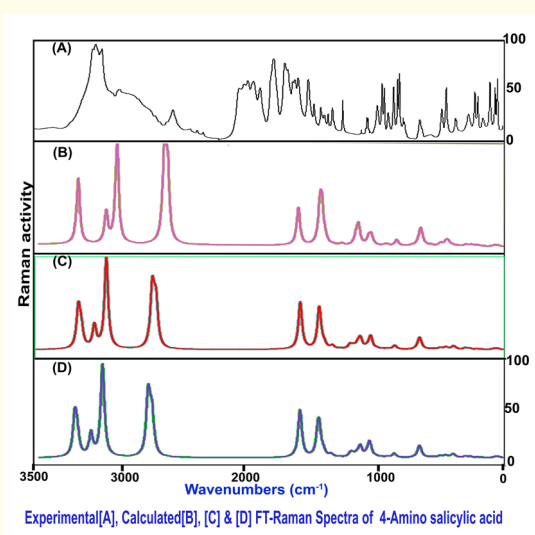

Experimental[A], Calculated[B], [C] & [D] FT-Raman Spectra of 4-Amino salicylic acid

C-H vibrational profile

Since the benzene base of title molecule was identified to be substituted by three different ligand groups, three C-H bonds were available to represent the base vibrations. The stretching modes of such bonds were observed strongly at 3000, 2990 and 2985 cm 1 in IR spectrum. Due to the occupation of such stretching in IR only, it proved that, the bonds possessed strong dipole character. According to the literatures [21,22], such vibrations are to be observed in the region 3100-3000 cm^{-1} for benzene derivatives. But, these vibrations were identified just below the expected region. Usually, the core stretching vibrations have hold back due to the suppression of substitutional vibrations and chemical effect of its surroundings. In this case, since the stretching vibrational energy was sucked by acid and amino groups, the core C-H stretching modes were affected. This view indicates that, the core was affected rather and simultaneously, the chemical effect of core was found to be distorted little bit in favor of ligand property.

The in plane and out of plane bending vibrations of C-H about hexagonal frame were purely observed at 1150, 1060 and 950^{-1} and 790, 780 and 750 cm^{-1} respectively. The in plane and out of plane bending vibrations usually found in the region 1300 - 1000 cm^{-1} and 1000 - 750 cm^{-1} respectively [23]. Accordingly, these vibrations have been found to be observed in lower end of the expected region which was also affected similar to the stretching. From these view, it was clear that, the core property was to be changed with respect to Amino and acid groups.

CC vibrations

The hexagonal core vibrations is significant to discuss because, it provides the information directly regarding the measurement scale of change of chemical property of complex molecule due to the substitutions. Here, since the core was injected by three different ligand groups, the frame was definitely affected and it can be determined from the dislocation of vibrational region of core vibrations. According to the literatures [24,25], the CC stretching vibrations are normally observed in the region 1650 - 1400 cm^{-1} for benzene derivatives. But, in this case, the C=C stretching modes were found at 1600, 1570 and 1550 cm^{-1} and C-C signals have been observed at 1530, 1510 and 1470 cm^{-1} respectively. All these vibrational modes were identified within the expected region and the entire wavenumbers were located at the center of the allowed range of spectrum. This surveillance of accurate presence of such vibrations is rarely taking place. So, in this case, the core was not offended much as expected. The ring breathing modes in terms of plane of molecule were found at 490, 410 and 360 cm^{-1} and 300, 280 and 210 cm^{-1} respectively. From these breathing modes, it was clear that, the ring deformations on both in plane and out of plane were found to be affected much due to the substitutional dominance.

Amino group vibrations

In primary aliphatic amines, the hydrogen bonding may absorb the infrared radiation in the region of 3160 - 3450 cm^{-1} [26,27]. In the diluted solution of molecular complex with non-polar solvents, two bands are observed for primary amines due to N-H asymmetric and symmetric stretching. In the aliphatic case, they are in the range 3550 - 3250 cm^{-1} whereas in the aromatic case, they are of medium intensity, one would be at 3520 - 3420 cm^{-1} and the other at 3420 - 3340 cm^{-1} [28-29]. Here, for the aromatic amine, the N-H stretching vibrational bands were found at 3300 and 3290 cm^{-1} which are available in region by which the bands could not be identified whether from aromatic or aliphatic. This untraceable state of vibrations was produced by the acid group since it is involved in the preparation of drug property along with the amine group.

Normally, primary aromatic amines produced the in plane bending modes in the region 1615 - 1580 cm^{-1} [30] and out of plane bending modes are observed at 1120 - 1020 cm^{-1} [31]. The in plane and out of plane bending modes were observed at 1390 and 1385 cm^{-1} and 855 and 850 cm^{-1} correspondingly. Similar to the stretching, these bending bands also affected due to the vibrational energy consumed partially. The C-N stretching band for aromatic and unsaturated amines is observed at 1360 - 1250 cm^{-1}.But in this saturated case, this signal was found at 1315 cm^{-1} and was hopefully observed within the limited region which represents the amine holding point of ring.

COOH group vibrations

By the efficient of strong intermolecular hydrogen bonding, the carboxylic acids normally survive as dimers. Tentatively, their spectra exhibit a broad band due to the O-H stretching vibration and a strong band due to the C=O stretching vibration. The remarked spectral modification which occur when a carboxylic acid is in the form of salt may be used to distinguish it from other C=O containing compounds.

As a result of the presence of hydrogen bonding, carboxylic acids in the liquid and solid phases exhibit a broad band at 3450 - 3300 cm^{-1} due to the O-H stretching vibration [32,33]. Concurrently, the C=O stretching signals are appeared at 1685 - 1640 cm^{-1} [33]. For the present compound, the O-H and C=O stretching modes were found at 3450 and 3445 cm^{-1} and 1610 cm^{-1} respectively. Here, the O-H vibrations were observed at the top end of the expected region whereas the C=O stretching was found well below the characteristic region. The corresponding in plane bending bands were found at 1450 and 1395 cm^{-1} and 840 cm^{-1} respectively. Similarly, the out of plane bending bands for O-H bond were found at 880 and 875 cm^{-1}. But, the O-H in plane and out of plane bending vibrations are allowed in the region 1440 - 1395 cm^{-1} and 970 - 875 cm^{-1} respectively [34]. Unlike to the stretching modes, the bending vibrational bands positioned at the bottom end of the limited region. This view showed the lower frequency energy of this N-H bond was shared by the C=O group for the enhancement of product property.

C-O vibrational observation

In this analytical molecule, the C-O bond was found at two different locations due to which their vibrational peaks were determined in two different regions. The vibrational wavenumber of the bond C-O directly related to ring was strongly found at 1250 cm^{-1} whereas the bond C-O linked with acid group was found with medium intensity at 1170 cm^{-1}. Actually, the C-O bond associated with carboxylic acid vibrations are usually observed in the region 1190-1075 cm^{-1} [35]. The first band was found within the allowed region whereas the second band was observed well above the expected region. This view displayed that, for the first case, the energy was neither conducted nor absorbed. For the second case, the energy was absorbed from the ring.

NMR analysis and observation

The observed and calculated chemical shift values were presented in the table 4 and the corresponding diagram shown in figure 6. Usually, the proton-chemical shifts on carbon in organic molecules fall in several distinct regions, depending on the nature of adjacent carbon atoms, and the substituents on those carbons. The ^{13}C is more complicated than proton-chemical shifts, which are primarily determined by diamagnetic and anisotropic shielding effects [36].

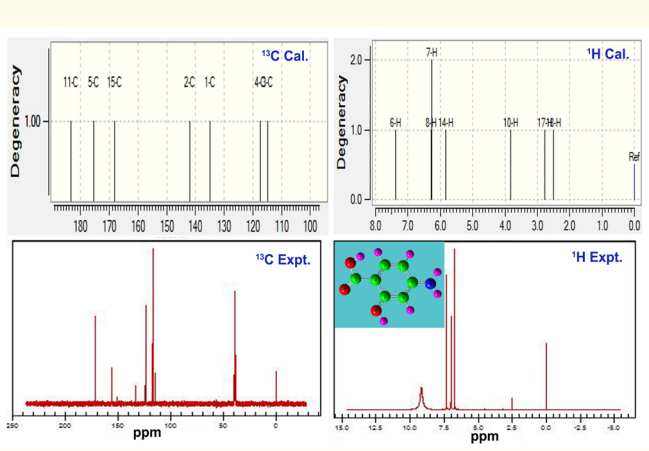

Atom position	TMS-B3LYP/6-311++G(2d,p) Shift (ppm)			Experimental shift (ppm)
	Gas	Solvent phase		
		DMSO	Chloroform	
C1	141.90	146.15	144.77	150
C2	134.85	132.68	133.34	133
C3	114.88	117.18	116.39	114
C4	117.44	119.73	119.02	117
C5	175.49	173.27	174.02	172
C11	183.39	188.31	186.82	179
C15	168.07	170.74	169.99	156
H6	7.37	7.83	7.68	-
H7	6.25	6.62	6.50	6.7
H8	6.25	6.74	6.60	6.6
H10	3.82	4.48	4.29	-
H14	5.83	6.85	6.50	6.5
H17	2.76	3.27	3.12	-
H18	2.50	3.05	2.89	2.5

Table 4: Experimental and calculated ^{1}H and ^{13}C NMR chemical shifts (ppm) of 4-Aminosalicylic acid.

The aromatic carbons, usually, having large chemical shift due to the substitutions and type of the same. If the electron-donating ligand is substituted on the ring, this will create electronegative. When the electron-withdrawing substituent is added on the ring carbon, this makes the carbon more electropositive. Concurrently, the distance from the nucleus to its p-electrons will decrease, increasing the paramagnetic deshielding. This means the carbon will have a larger chemical shift which explains why many carbon chemical shift tendency parallel the diamagnetic influence used for proton.

Here, in the present compound, the ring was substituted by amine, Acid and hydroxyl groups where the associated carbons having different chemical environments. Thus, the alternation of chemical property of benzene ring with respect to substituents can be measured by the respective chemical shifts. The carbons in the ring free from substitutions, C2, C3 and C4 having the chemical shift; 134, 114 and 117 ppm respectively. Except C2, the rest of carbons were having moderate chemical shift as it was expected. The excess of chemical shift of C2 was due to the extension of electron cloud from up to C2. This trend was observed in Mulliken charge analysis by large negativity on C2 as C1. At the substitutional place, the carbon C5 (Expt. 175 ppm and Cal.172 ppm) has more shifted than C15 (Expt. 156 ppm and Cal.168 ppm) which has greater shift than C1 (Expt. 141 ppm and Cal.133 ppm). Since the ring has much affected by hydroxyl group by random breaking of shield of carbon, the hydroxyl group plays vital role in making drug property. Usually, the amine group is always having dominating character which was observed in vibrational analysis. Such as amine group affected the ring much by producing large chemical shift on substituted carbon by which it was clear that, the amine group in para position emphasize its partial involvement for the inducement of drug property. Then, the acid group at carbon C1 due to which the moderate chemical shift was identified. This showed the intermediate contribution on incentive of chemical property. The carbon C11 at acid group was much more shifted than any other carbons in the molecule which ensured electrophilic influence of C=O. In the case of proton chemical shift, the ring H has large shift than amine group H which has greater than hydroxyl H. From this discussion, it was concluded that, the electron withdrawing groups make intensive effect on ring than donating group and this mechanism was the source of such drug activity on molecule.

Frontier molecular interaction study

The frontier molecular levels with values were presented in table 5 and the diagram shown in figure 7. The modern molecular orbital theory is tentatively used by chemists to illustrate the arrangement of electrons in different energy levels on chemical structures. It provides theory basis for elucidating the ground-state shapes of molecules and their many other properties [37]. The Molecular orbital theory is related with bonding and non-bonding profile of orbitals and capable of giving some insight into the chemical forces involved in the making and breaking of chemical bonds.

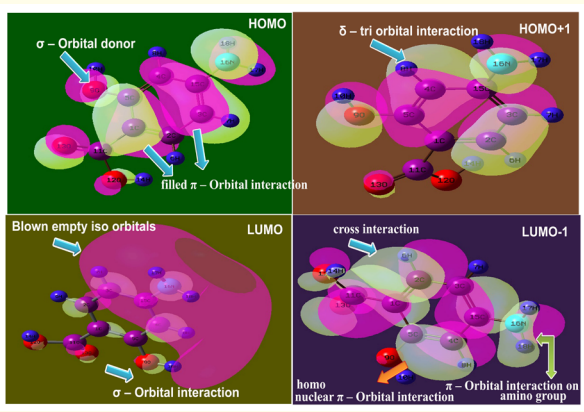

Energy levels	Frequency region B3LYP/6-311++G(d,p) (eV)	UV-Visible region (eV)
H+10	11.7515	11.4464
H+9	11.3993	11.1982
H+8	10.8037	10.9163
H+7	10.6195	10.4407
H+6	10.5525	10.2989
H+5	10.229	9.8826
H+4	8.9560	8.9979
H+3	8.5721	8.6709
H+2	7.4844	7.4752
H+1	7.0169	7.2330
H	6.2988	6.7018
L	1.1877	1.9105
L-1	0.7545	1.0702
L-2	0.7148	0.7387
L-3	0.3776	0.4900
L-4	0.2511	0.2742
L-5	0.2544	0.2144
L-6	0.5415	0.3542
L-7	0.7559	0.6696
L-8	1.0911	1.0236
L-9	1.1964	1.1325
L-10	1.5020	1.4604

Table 5: Frontier molecular orbital's of 4-Aminosalicylic acid with energy levels.

The perturbation theory on setting up of molecular orbitals and account on transitions among molecular orbitals is enforced to deliberate molecular interaction among the degenerate orbitals for the better understanding of cascading of both occupied and unoccupied molecular orbitals. The reactivity of molecular product-complex is enforced by the arrangement of interactive orbitals and the occurring of transitional energy. The utilized energies among molecular interaction is obviously important for explaining the mechanism constructed for creating desired chemical activity.

In order to explain the type of chemical reaction for inducing such peculiar chemical property, it is necessary to analyze the system of HOMO and LUMO energy structure. Here, the available electronic energy orbitals concentrated as π-bond interaction on semicircle carbons of ring on amine and acid group side. The σ-orbital non-interactive donor obtained over O of hydroxyl and

acid groups. In HOMO+1 array of orbitals, δ-tri-orbitals interactions forced to accumulate the electrons for semicircle of ring on the side of hydroxyl and amine groups. But here, the σ* (non-bonding) orbitals were found on O and N where rather not as much of energized electrons are obtained for making transitions. Thus, the chemical energies have been filled up in terms of electronic energy for making transitions for producing chemical property.

In empty orbital side (LUMO), the positive isosurface is uncertainly separately present over carbons, Nitrogen and Oxygen atoms of entire molecular system whereas the negative isosurface was found to be identified as blown orbital which covered the top moiety of the ring, hydroxyl group and amino group and this arrangement has been considered as multi degenerate energy level coordination system. These overlapped spacial orbitals were treated as centralized orbitals which received the electrons under transitions from occupied orbitals. The revolving electrons in interacted orbitals system were causing the amalgamation of chemical property of all ligands with ring. In second order orbital level (LUMO-1), there were homo nuclear and hetero nuclear interaction orbitals (π-orbital overlapping) found on C=C of the ring, C=O and NH_2 components. In addition to that, the cross orbital π-interactions were identified between ring C and COOH groups and C=C-O-H group. This means that, the electrons under transitions from HOMO were shared by ring COOH group which was also for integration of chemical property.

CT complex profile analysis in UV-Visible spectra

The excitation analytical values for electronic structure of 4-Aminosalicylic acid was presented in the table 6 and associated CT absorption graph for experimental and calculated were revealed in figure 8. Usually, the region of electronic absorption band of aromatic compound is depends upon the presence of functional parts; chromophores and auxochrome [38]. Such an operating part in molecular system called CT complex which is very significant in UV-Visible spectra since it provides the information regarding components which is source of chemical reactivity entity which is the root cause of the (drug activity) [39].

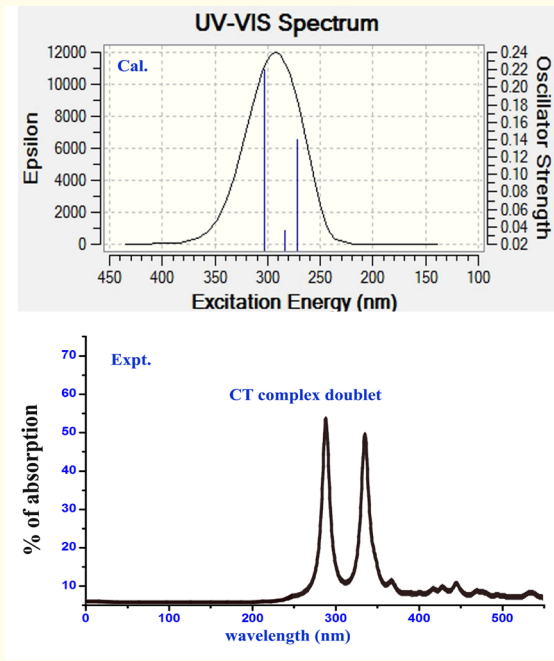

λ (nm)	E (eV)	(*f*)	Major contribution	Assignment	Region	Bands
Gas						
305.89	4.1205	0.0104	H+2→L (56%)	n→π*	Quartz UV	R-band (German, radikalartig)
270.8	4.2688	0.127	H+2→L (59%)	n→π*		
262.00	4.7323	0.061	H+2→L (22%) H+1→L (52%)	n→π*		
DMSO						
305.94	4.0526	0.2329	H+2→L (64%)	n→π*	Quartz UV	R-band (German, radikalartig)
280.02	4.4277	0.0960	H+2→L (46%)	n→π*		
272.46	4.5505	0.0754	H+2→L (50%)	n→π*		
Chloroform						
302.65	4.0967	0.2205	H→L (64%)	n→π*	Quartz UV	R-band (German, radikalartig)
283.85	4.3680	0.0349	H+2→L (62%)	n→π*		
271.22	4.5714	0.1399	H+2→L (62%)	n→π*		

Table 6: Electronic absorption spectra of 4-Aminosalicylic acid (absorption wavelength λ (nm), excitation energies E (eV) and oscillator strengths (f)) using TD-DFT/B3LYP/6-311++G(d,p) method.

Normally, the base is reacted with ligands which may be chromophores or auxochrome forms complex. In this molecule, the chromophores were found to be C=C, C-C, C-N and C=O and auxochromes were identified to be amino group and hydroxyl group. Due to the interaction between Donor (Lewis base) and acceptor (Lewis acid), the CT complex was produced. In this aromatic complex, the charge transfer complex is generated which may cause the inducement of new biological or pharmaceutical property. The property can be measured by measuring the electronic excitation absorption wavelength in the UV-Visible spectrum.

According to the combinations of chromophores and auxochromes, the CT complex was found to be amine and hydroxyl groups. Here, the charge transformation taking place from CT complex to the ring which was recognized by the absorption doublet peaks noted at 290 and 340 nm in experimental spectra and consequently, the calculated wavelength observed at 270 and 305 nm. The absorption band represented as n→π* transition in gas phase was noted at 305 and 270 with the energy gap of 4.1 and 4.2 eV respectively for the oscillator strength of 0.01 and 0.12 respectively. The transition band was identified as R-band (German, radikalartig) and the spectral region was Quartz UV. In DMSO solvent, the transitions were observed at 305 and 280 nm with the energy gap of 4.0 and 4.4 eV with the oscillator strength of 0.23 and 0.09 which was consistently assigned from HOMO to LUMO-1. From the discussion, it was infer that, the transitions for CT complex designated as n→σ* by amine and hydroxyl group and n→π* was attained by C=O group. Normally, if CT complex absorption band located at quartz UV region, the compound will be biologically active. Obviously, these two CT complex was the reason for the present compound to be the antibiotic drug.

Molecular electrostatic potential (MESP) maps

The chemical bond in organic compounds usually results from the redistribution of charge density in the binding region to an extent sufficient to balance the equilibrium chemical forces of attraction and repulsion. The covalent binding signified by two possible opposite charge boundaries of reaching this state of electrostatic symmetry and the absolute spectrum of bond densities lying between these two limits. Since covalent charge distributions exhibit radically different chemical and physical properties, it is significant that, most closely approximates of boundaries of binding of molecule. The charge density is unequally shared by the nuclei in the molecule for the maintenance of equilibrium potential among the atoms used to measure the physical and chemical property.

The 3D electrostatic potential map of the title compound was portrayed in between the existence of positive and negative potential contours in figure 9. Here, for the present molecule, the MESP has been plotted in which the value was identified to be ± 8.411 e^{-2}. This was relatively high to recognize the ligands with benzene ring. The positive potential zone was located over hydroxyl and acid groups where the electron cloud was sucked by these groups from the ring whereas the protonic region was identified mainly over amino group and hydrogen region of the molecule. The intermediate zone called neutral region which were sited at C-H bonds of left and right moiety. The region from acid group to ring C-H the electron dislocation was faded and appeared as yellow region.

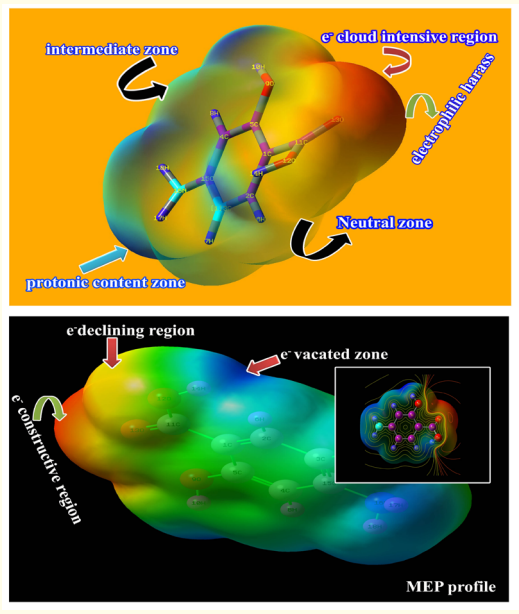

Generally, the amine group is treated as electron withdrawing group and the negative zone should be placed around amine group. But here, by the dislocation of electron intensive sector from amino to ring, the amine group was appeared as positive potential region. This electron cloud push by amino group and pull by acid and hydroxyl group making the molecule very strong and enhanced dipole character. Such a mono dipole enticement on molecule by the ligand group's results highly polar character which was very noteworthy to produce the specific chemical potential to fascinate the antibiotic property on molecule.

Exploration of Physico-chemical properties

The atomic orbitals are usually modified as molecular orbitals which depleted in to donor and acceptor within the molecule. The depleted molecular orbitals limited by two sets usually named as HOMO and LUMO and they are arranged irrespective of base and ligands. The energy gap devoted between filled and empty orbitals indirectly helped to calculate all known parameters which replicate the quantity of chemical property and thereby the application of the compound tend to predict. The calculated parameters were exhibited in the table 7.

Parameter	IR region	UV-Visible	Electrophilicity charge transfer (E_{CT}) $(\Delta N_{max})_A$-$(\Delta N_{max})_B$
E_{total} (Hartree)	-607.660	-551.349	
E_{HOMO} (eV)	7.2077	6.701	
E_{LUMO} (eV)	1.138	1.910	
$\Delta E_{HOMO\text{-}LUMO\ gap}$ (eV)	6.069	4.791	
$E_{HOMO\text{-}1}$ (eV)	7.365	7.233	+ 1.96
E_{LUMO+1} (eV)	0.683	1.070	
$\Delta E_{HOMO\text{-}1\text{-}LUMO+1\ gap}$ (eV)	6.682	6.162	
Chemical hardness (η)	3.034	2.395	
Electronegativity (χ)	4.173	4.306	
Chemical potential (μ)	4.173	4.306	
Chemical softness(S)	-12.13	-9.582	
Electrophilicity index (ω)	2.869	3.870	
Dipole moment	7.935	6.732	
ETC	2.754	2.500	

Table 7: Calculated physico-chemical parameters of 4-Aminosalicylic acid.

The zero point vibrational energy of present molecule was in IR and UV-Visible region was found to be -607.66 and -551.34 Kcal/mol respectively. The energy required to bind molecule in UV-Visible region was found to be greater than IR region which showed the compound was more reactive in UV-Visible region than IR region. The dipole moment of the title molecule was found to be 7.93 and 6.73 dyne in IR and UV-visible region respectively. The resultant dipole moment is used to measure the aptitude of charge depletion in terms of polarization of molecule. As it was more in this case than aromatic measurement unit, the present molecule was much reactive and has consistent chemical rigidity.

The chemical hardness is the measure of resistance ability of chemical substance to modify its electronic configuration [40] which is also used to indicate the chemical reactivity and stability [41]. Here, it was calculated to be 3.03 and 2.39 eV in IR and UV-Visible region respectively. According to the literature, the present compound has consistent electronic structure and it will never change itself by nearby chemical species. Also has moderate chemical stability. The ionization potential is a scale of indicator which is used to measure resultant chemical reactive energy with existed filled energy levels [42]. The ionization potential is observed to be 4.173 and 4.306. Accordingly, the observed values were not absolutely less which was effortful to sustain the stabilized chemical reactive energy in molecular orbital spot.

The Electronegativity is a gauge of attraction of electron clouds by particular species or entities of complex molecule. Usually, the local electro-chemical forces on particular nuclei have an ability to attract the electrons irrespective of its polarity in molecule. Such a accumulation on entity was the basis for core property of the molecule. In this case, the same was found to be 4.17 and 4.30 in IR and UV region respectively. The observed values were caused by ligand groups in base ring which was adequate to attach with protein complex with minimum energy. This electronegativity of the whole structure was guided by π- bond (C=O) and σ-bond interactions and was ensured in MEP view.

The electrophilicity index is used to estimate of rate of flow of chemical potential energy between the ligand and base of the compound. The electrophilicity index ω measures the energy lowering of a ligand due to maximal electron flow between donor and acceptor [43]. In this case, the electrophilicity index is 2.86 and 3.87 eV in IR and UV-Visible region respectively and the Electrophilicity charge transfer was determined to be 1.96. The energy flow mechanism constructed during the amalgamation of complex molecule. Here, the mechanism was found to be constructed for unidirectional energy flow from base ring to ligand. The mono directivity of chemical energy was obviously confirmed from the electrophilicity charge transfer which was found to be + 2.81 for present molecule and it was ensured that, considerable amount of energy was exchanged from ring to ligand and the energy was utilized to persuade the antibiotic activity.

Polarization and Hyper polarization analysis

The interactions between polar non-polar atoms and molecules lead polarization and basically the atoms and molecules are electrically charged species acquired dipoles. During the formation of molecule, at the point of electric field, the charged polar or non-polar atoms combined and also the electrons loosely bonded with other charged atoms. Thus, the redistribution of electrons in the atomic sites produced the strong polarization in first order and second order. The atoms of base and ligand groups placed in different coordinate systems combined to structure the molecule in different planes which are synchronized with the polarization of two orders. Such polarizations directing the electron and produced charged path for displacement of chemical potential from one entity to other within the molecule [44]. The coefficient of polarization and hyperpolarization is employed to identify the orientation of chemical energy for generating chemical property.

All types of computed Polarizability and first order hyperpolarizability indices were depicted in table 8. Here, the calculated average Polarizability and anisotropy of the Polarizability of the present compound was 144 x 10^{-30} esu and 218 x 10^{-30} esu respectively and the hyperpolarizability (β) was found to be 65.88 x 10^{-33} esu. Usually, the average value always lesser than anisotropy coefficient since the anisotropy polarization is independent of coordinate system. Here, the main source of polarization was found to be started from ring to COOH and OH groups and thus the root was clear for generating the chemical potential for producing anti-mycobacterial agent. The hyper Polarizability also known as second order polarization order which is independent of first order and it was found to be high. This type of high degree of hyper action was the root cause of anti-tuberculosis activity.

Parameter	a.u.	Parameter	a.u.
$_{\alpha x}$x	-67.1964	β_{xxx}	-103.1044
α_{xy}	-4.7285	β_{xxy}	-5.7303
α_{yy}	-50.9577	β_{xyy}	-15.7481
α_{xz}	0.0676	β_{yyy}	19.6556
α_{yz}	0.9587	β_{xxz}	23.8106
α_{zz}	-66.4899	β_{xyz}	-1.6713
α_{tot}	144.447	β_{yyz}	6.3979
Δα	218.378	β_{xzz}	11.3553
μ_x	-7.5058	β_{yzz}	-0.7523
μ_y	-0.7009	β_{zzz}	4.8101
μ_z	2.4777	β_{tot}	65.8866
μ	7.9352		

Table 8: The dipole moments μ (D), the polarizability α (a.u.), the average polarizability αo (esu), the anisotropy of the polarizability Δα (esu), and the first hyperpolarizability β (esu) of 4-Aminosalicylic acid.

NBMO analysis

After the arrangement of hybridization of molecular orbitals, the electronic energy absorbed by the complex system is utilized for the transitions among different energy levels of non-bonding molecular orbitals. The perturbed degenerate energy levels sharing such kind of energy between occupied Lewis type (bond or lone pair) orbitals and unoccupied (anti-bonding and Rydberg) non-Lewis orbital in order to stabilize donor acceptor interaction for creating molecular mechanism for manipulating drug property [45]. The important donors and acceptors of interacted electronic orbitals were recognized and their energy transitions were obtained. The transitions on different entities of the molecule were presented in table 9.

Donor (i)	Type of bond	Occupancy	Acceptor (j)	Type of bond	E2 kcal/mol	Ej – Ei au	F(I j) au
C1-C2	π	1.97927	**C3**	π*	1.65	1.76	0.048
	σ		**C1-C5**	σ *	2.36	1.14	0.047
	π		**C2-C3**	π*	1.60	1.15	0.038
	π		**C5-O9**	π*	2.31	1.02	0.043
	π		**C3-C15**	π*	8.01	0.31	0.045
	π		**C4-C5**	π*	12.15	0.31	0.055
	π		**C11-O13**	σ *	17.29	0.29	0.063
C1-C5	σ	1.96960	**C4**	σ *	1.89	1.50	0.048
	σ	1.96960	**C1-C2**	σ *	2.66	1.26	0.052
	σ		**C2-H6**	σ *	2.80	1.09	0.050
	σ		**C4-C5**	σ *	2.06	1.25	0.045
	σ		**C4 -H 8**	σ *	2.74	1.08	0.049
	σ		**C11-O12**	σ *	2.07	0.90	0.039
C1-C11	σ		**C1-C2**	σ *	2.17	1.27	0.047
	σ		**C4-C5**	σ *	3.74	1.04	0.056
C2-C3	σ	1.97256	**C1**	σ *	2.34	1.81	0.058
	σ		**C15**	σ *	2.32	1.80	0.058
	σ		**C1-C 2**	σ *	2.07	1.24	0.045
	σ		**C1-C11**	σ *	4.10	0.99	0.057
	σ		**C3-C15**	σ *	2.14	1.24	0.046
	σ		**C15-N16**	σ *	5.22	0.95	0.063
C2-H 6	σ	1.97866	**C1**	σ *	1.79	1.71	0.050
	σ		**C1-C 5**	σ *	5.83	0.94	0.066
	σ		**C 3-C15**	σ *	1.51	1.18	0.038
	σ		**C3-C15**	σ *	1.51	1.18	0.038
C3-H 7	σ	1.97892	**C15**	σ *	1.87	1.55	0.048
	σ		**C1-C 2**	σ *	1.75	1.15	0.040
	σ		**C3-C15**	σ *	1.57	1.16	0.038
	σ		**C 4-C15**	π*	6.05	0.92	0.067
C3-C15	π	1.78300	**C2-C3**	π*	1.70	1.15	0.039
	π		**C4-C15**	π*	1.95	1.14	0.042
	π		**C1-C2**	π*	13.49	0.30	0.058
	π		**C4-C5**	π*	8.47	0.30	0.045
C4 -C 5	π	1.98322	**C1**	π*	1.68	1.91	0.051
	π		**C1-C5**	π*	2.39	1.15	0.047
	π		**C1-C11**	π*	1.53	1.13	0.038
	π		**C4-H8**	π*	1.55	1.20	0.039
	π		**C4-C15**	π*	1.83	1.15	0.041
	π		**C15-N16**	π*	2.22	1.09	0.044
	π		**C1-C2**	π*	9.08	0.31	0.048
C4-H8	σ	1.97744	**C1-C5**	σ *	12.96	0.31	0.058
	σ		**C1-C5**	σ *	5.48	0.93	0.064
	σ		**C3-C15**	σ *	2.29	1.17	0.046
	σ		**C4-C5**	σ *	1.58	1.16	0.038
C4-C15	σ	1.96959	**C3-H 7**	σ *	2.98	1.09	0.051
	σ		**C3-C15**	σ *	2.25	1.26	0.048
	σ		**C4-C 5**	σ *	1.88	1.24	0.043
	σ		**C5-O 9**	σ *	4.83	0.90	0.059
	σ		**C4-C15**	σ *	2.18	1.23	0.046
	σ		**C5**	σ *	2.70	1.74	0.061
C5-O9	σ	1.99254	**C1-C5**	σ *	3.70	1.12	0.058
C11-O13	π	1.99530	**C1-C 2**	π*	4.78	0.38	0.041

O12- H14	σ		**C11-O 13**	σ *	1.61	0.75	0.033
C15 -N16	σ	1.99096	**C2-C3**	σ *	2.67	1.14	0.049
N16-H17	σ	1.98593	**C4-C 15**	σ *	3.75	1.04	0.056
N16-H18	σ		**C3-C15**	σ *	3.07	1.27	0.056
N16-H18	σ	1.98642	**C3-C15**	σ *	1.94	10.96	0.130
C2	LP	1.99902	**C1**	N*	1.86	11.21	0.129
C5	LP		**C4-C5**	π	1.89	10.74	0.128
O9	LP	1.99976	**C5-O9**	σ	1.64	10.39	0.117
O 9	LP		**C 5**	N*	1.76	19.94	0.168
O13	LP	1.99977	**C11**	N*	5.73	19.85	0.302
C15	LP	1.99895	**C3**	N*	2.23	11.11	0.141
C15	LP		**C3-C15**	π	1.57	10.73	0.116
N16	LP	1.99946	**C15**	N*	1.67	15.16	0.142
O9	LP		**C 5**	N*	2.11	1.61	0.052
O9	LP		**C4-C5**	π	4.49	1.21	0.066
O9	LP		**C4-C5**	π	20.27	0.35	0.078
O12	LP	1.97537	**C1-C11**	σ	4.88	1.00	0.063
O12	LP		**C11-O13**	π	2.42	0.87	0.042
O12	LP		**C11- O13**		24.28	0.34	0.083
O13	LP	1.98160	**C11**	N*	13.81	1.71	0.137
O13	LP		**C1-C11**	σ	14.48	0.61	0.086
O13	LP		**C11-O12**	σ	31.16	0.50	0.113
N16	LP	1.87516	**C3-C15**	π	17.38	0.37	0.074
C11–O12	σ		**C 1-C2**	π	51.36	0.02	0.063

Table 9: The calculated NBO of 4-Aminosalicylic acid by second order Perturbation theory.

Here, the numerous transitions among different donor and acceptor bonds and lone pairs were acknowledged which were causing concluded property. In the ring, the electronic energy of 8.01 kcal/mol was transferred from C1-C2 to C3-C15. Similarly, the potential energy of 12.15 and 17.95 kcal/mol found to be exchanged between C1-C2 and C4-C5 and C11-O13 with the occupied energy of 1.97 au which was assigned by π - π * interaction system. In this case, the energy from single source was transferred to acid as well as amino group.

The energy of 13.49 and 8.47 kcal/mol were transferred from C3-C15 to C1-C2 and C4-C5 respectively which were assigned as π - π * interaction system. Similarly, the energy of 12.96 kcal/mol was found to be transferred from C4-H8 to C1-C5 and was assigned as π - π *. Another transition has been observed from lone pair O9 to C4-C5 in which 20.27 kcal/mol of energy was used for σ-σ*. The important transition was found to be observed for exchanging energy from OH to ring. The transitions were found from O12 to C11-O13 and O13 to C11 with 24.2 and 13.8 kcal/mol of energy which were assigned to LP- π interaction system. The transitions O3 to C1-C11 and C11-O12 were observed for taking energy of 14.4 and 31.3 kcal/mol from COOH to the ring. Similarly, the transitions N16 to C3-C15 and C1-C2 by consuming 17.3 and 51.3 kcal/mol of energy and was assigned as σ-σ*. Other than these transitions, there were number of interactional transitions have been identified and observed with feeble amount of energy. From this observation, it was concluded that, the unbounded electrons from atoms without bonding as well as lone pair were found to be participated to exchange of chemical energy between base to ligands and vice versa., for constructing drug potential. Here, the entire occupation of ligand groups were involved themselves to circuit the root cannel path for the hyper polarization to arrange the consistent antibiotic property.

VCD profile

The simulated VCD spectrum of present molecule was displayed in the figure 10 which ensured that, the compound under study was optically active as well as biological active. The VCD in the molecules usually is simulated by the presence of dextrorotary and levorotary components. The spectral signature produced by the vibrational process occurred within the biological molecules are able to generate secondary wavenumbers by which the secondary structure can be constructed. If this structure similar to the primary structure, the secondary one will be the enantiomer. The spectral sequence in mid over and above near infrared region was identified to be same which ensured that, the compound was not necessary to filter the unusual property. The toxic effect was not essentially hidden and the compound was determined to be pure. In addition to that, the amino progression in the spectrum was clear whereas the acid group was least puzzled. Though COOH have produced sketched defect on spectral pattern, it was partially inactive participation in property fascination. The spectral region related to base compound was found to be very clear which was ensured that, the base has not produced any VCD defect on this system.

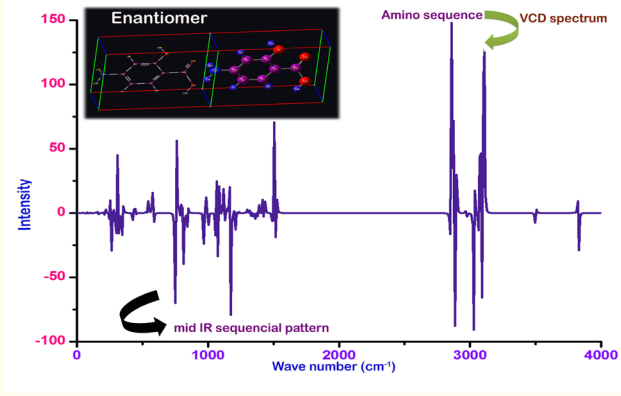

Conclusion

The molecular spectroscopic and theoretical tools were properly used to predict the physical, chemical and biological properties of the present compound; 4-Aminosalicylic acid. The stable structure was optimized by performing scanning process. The reconstructed structural parameters were tabulated and change of bond length and bond angle were profoundly analyzed. Due to the attachment of active ligands in ortho, meta and para positions in benzene ring, the change of molecular activity was analyzed. The asymmetric charge delocalization in different entities of the molecule was eagerly measured and the orientation of electron potential with respect to substitutions causing the molecular reactivity was investigated. The arrangement chemical reaction path among entire carbons was ensured by the proper site of chemical shift was conferred. The chemical process linked with lobe interaction for orbiting hybrid electrons to produce desirable drug property was predicted from the degenerate frontier molecular orbitals.

Bibliography

1. P Wen., *et al*. "Salicylic acid activates phenylalanine ammonia-lyase in grape berry in response to high temperature stress". *Plant Growth Regulation* 55.1 (2008): 1-10.

2. YP Singh., *et al*. "Numerical simulation of the internal vibrations of COOH group in amino-salicylic acids". *African Journal of Biochemistry Research* 1.2 (2007): 19-23.

3. MK Jain and SC Sharma. "Organic Chemistry". Shoban Lal Nagin Chand and Company, Educational Publishers, New Delhi (1980).

4. Botella GM., *et al*. "Discovery of Selective and Potent Inhibitors of Gram-Positive Bacterial Thymidylate Kinase (TMK)". Journal of Medicinal Chemistry 55.22 (2012): 10010-10021.

5. S Ramalingam., *et al*. "FTIR and FTRaman spectroscopic investigation of 2-bromo-4-methylaniline using ab initio HF and DFT calculations". *Spectrochimica Acta Part A: Molecular and Biomolecular Spectroscopy* 76.1 (2010): 84-92.

6. C Yohannan Panicker., *et al*. "FT-IR, FT-Raman and FT-SERS spectra of 4-aminosalicylic acid sodium salt dihydrate". *Spectrochimica Acta Part A* 58.2 (2002): 281-287.

7. Humberto C Garcia., *et al*. "Co-crystal and crystal: Supramolecular arrangement obtained from 4-aminosalicylic acid, bpa ligand and cobalt ion". *Journal of Molecular Structure* 1010 (2012): 104-110.

8. D Braga., *et al*. "Drug-containing coordination and hydrogen bonding networks obtained mechanochemically". *CrystEngComm* 11 (2009): 2618-2621.

9. N Moorthy, *et al*. "Vibrational, NMR and UV–visible spectroscopic investigation and NLO studies on benzaldehyde thiosemicarbazone using computational calculations". *Journal of Physics and Chemistry of Solids* 91 (2016): 55-68.

10. S Xavier and S Periandy. "Spectroscopic (FT-IR, FT-Raman, UV and NMR) investigation on 1-phenyl-2-nitropropene by quantum computational calculations". *Spectrochimica Acta Part A: Molecular and Biomolecular Spectroscopy* 149 (2015): 216-230.

11. N Moorthy., *et al*. "Spectroscopic analysis, AIM, NLO and VCD investigations of acetaldehyde thiosemicarbazone using quantum mechanical simulations". *Journal of Physics and Chemistry of Solids* 95 (2016): 74-88.

12. A Madanagopal., *et al*. "Molecular structure activity on pharmaceutical applications of Phenacetin using spectroscopic investigation". *Journal of Molecular Structure* 1127 (2017): 611-625.

13. S Ramalingam., *et al*. "Vibrational investigation, molecular orbital studies and molecular electrostatic potential map analysis on 3-chlorobenzoic acid using hybrid computational calculations". *Spectrochimica Acta Part A: Molecular and Biomolecular Spectroscopy* 84.1 (2011): 210-220.

14. P David Suresh Babu., *et al*. "Vibrational spectroscopic (FTIR and FTRaman) investigation using ab initio (HF) and DFT (LSDA and B3LYP) analysis on the structure of Toluic acid". *Spectrochimica Acta Part A: Molecular and Biomolecular Spectroscopy* 78.4 (2011): 1321-1328.

15. C Dykstra., *et al*. "Theory and Applications of Computational Chemistry, The First Forty Years". Chapter 13 (2005): 291-372.

16. M Khoshneviszadeh, *et al*. "Structure-based design, synthesis, molecular docking study and biological evaluation of 1,2,4-triazine derivatives acting as COX/15-LOX inhibitors with antioxidant activities". *Enzyme Inhibitor and Medicinal Chemistry* 31.6 (2016): 1602-1611.

17. CA Lipinski., *et al*. "Experimental and computational approaches to estimate solubility and permeability in drug discovery and development settings". *Advanced drug Delivery Review* 23.1-3 (1997): 3-25.

18. Mithun Rudrapal., *et al*. "Novel series of 1,2,4-trioxane derivatives as antimalarial agents". *Journal of Enzyme Inhibition and Medicinal Chemistry* 32.1 (2017): 1159-1173.

19. HM Faidallah., *et al*. "Synthesis and biological evaluation of fluoropyrazolesulfonylurea and thiourea derivatives as possible antidiabetic agents". *Journal of Enzyme Inhibition and Medicinal Chemistry* 31.1 (2016): 157-163.

20. M Khoshneviszadeh., *et al*. "Structure-based design, synthesis, molecular docking study and biological evaluation of 1,2,4-triazine derivatives acting as COX/15-LOX inhibitors with antioxidant activities". *Journal of Enzyme Inhibition and Medicinal Chemistry* 31.6 (2016): 1602-1611.

21. George Socrates. "Infrared and Raman Characteristic Group Frequencies (Tables and Charts)". John Wiley & Sons, Ltd (2001).

22. G Varsanyi. "Assignments of Vibrational Spectra of 700 Benzene Derivatives". Wiley, New York (1974).

23. D Mahadevan., *et al*. "Vibrational spectroscopy (FTIR and FTRaman) investigation using ab initio (HF) and DFT (B3LYP) calculations on the structure of 3-Bromo phenol". *Spectrochimica Acta. Part A, Molecular and Biomolecular Spectroscopy* 78.2 (2011): 575-581.

24. S Jeyavijayan and M Arivazhagan. "Study of density functional theory and vibrational spectra of hypoxanthine". *Indian Journal of Pure and Applied Physics* 48 (2010): 869-874.

25. D Sajan., *et al*. "Structural and electronic contributions to hyperpolarizability in methyl p-hydroxy benzoate". *Journal of Molecular Structure* 785.1-3 (2006): 43-53.

26. Bellamy and RL Williams. "The NH stretching frequencies of primary amines". *Spectrochimica Acta* 9 (1957): 341.

27. EV Titov and MV Poddubnaya. Tear. Eksp Khim 8 (1972): 276.

28. HJ Bernslein. "The average XH stretching frequency as a measure of XH bond properties". *Spectrochimica Acta* 18.2 (1962): 161-170.

29. WJ Orville-Thomas., *et al*. "208. NH_2-stretching frequencies in primary amines". *Journal of the Chemical Society* (1958): 1047.

30. CJ Pouchert. "The Aldrich Library of FTIR Spectra". The Aldrich Co. (1985).

31. K Ohno., *et al*. "Vibrational spectra and molecular conformation of taurine and its related compounds". *Journal of Molecular Structure* 268.1-3 (1992): 41-50.

32. M Oki and M Hirota. "Intramolecular Hydrogen Bonding in α-Keto- and α-Alkoxy-carboxylic Acids. VI. Substituent Effects on the Energy of the Hydrogen Bonding in α-Alkoxy- and α-Aryloxyacetic Acids". *Bulletin of the Chemical Society of Japan* 36.3 (1963): 290-296.

33. M Josien., *et al*. Cornpt. Rend., 250 (1960): 4146.

34. JW Brasch., *et al*. "Chemical Far Infrared Spectroscopy". *Applied Spectroscopy Reviews* 1.2 (1968): 187-235.

35. MK Hargreaves and EA Stevenson. *Spectrochimica Acta* 21 (1965): 1681.

36. JB Lambert and EP Mazzola. "Nuclear Magnetic Resonance Spectroscopy". Prentice-Hall (Chapter 3) (2004).

37. Ian Fleming. "Molecular orbitals and organic chemical reactions". University of Cambridge, UK, John Wiley & Sons Ltd (2010).

38. Nessreen A Al-Hashimi and Yasser HA Hussein. "Ab initio study on the formation of triiodide CT complex from the reaction of iodine with 2,3-diaminopyridine". *Spectrochimica Acta Part A* 75.1 (2010) 198-202.

39. RS Mulliken. "Molecular Compounds and their Spectra. II". *Journal of American Chemical Society* 74.3 (1952): 811-824.

40. RG Parr and W.Yang. "Density Functional theory of Atoms and Molecules". Oxford University Press: Oxford, (1989).

41. Guy Makov. "Chemical Hardness in Density Functional Theory". *Journal of Physical Chemistry* 99.23 (1995): 9337-9339.

42. CE Moore. "Ionization Potentials and Ionization Limits Derived From the Analysis of Optical Spectra". NSRDS-NBS 34. Washington, DC (1970).

43. Robert G Parr., *et al*. "Electrophilicity Index". *Journal of the American Chemical Society* 121.9 (1999): 1922-1924.

44. Petrucci Ralph H., *et al*. "General Chemistry, Principles and Modern Applications". Upper Saddle River, NJ: Prentice Hall (2007).

45. Myung-Hwan Whangbo. "Theory and Applications of Computational Chemistry: The First Forty Years". Edited by C Dykstra., *et al*. Chapter 26 (2015).

Volume 2 Issue 1 January 2018